Canadian Conference - Pacific Conference on Earthquake Engineering 2023
Vancouver, British Columbia
June 25th – June 30th, 2023

Surrogate modelling for seismic collapse risk assessment of steel moment resisting frames

Nenad Bijelić[1*], Andronikos Skiadopoulos[1] and Dimitrios G. Lignos[2]

[1] Postdoctoral Researcher, Resilient Steel Structures Laboratory, Civil Engineering Institute, École Polytechnique Fédérale de Lausanne (EPFL), Lausanne, Switzerland
[2] Full Professor, Resilient Steel Structures Laboratory, Civil Engineering Institute, École Polytechnique Fédérale de Lausanne (EPFL), Lausanne, Switzerland
[*]nenad.bijelic@epfl.ch (Corresponding Author)

ABSTRACT

With the overall goal of reducing the numerical burden of uncertainty quantification involved in seismic risk assessments, this paper examines opportunities for assessment of seismic collapse capacity and risk using data-driven surrogates as a complement to physics-based response history analyses. Specifically, a methodology is proposed for computing collapse fragilities for generic sets of earthquake ground motions (i.e., not hazard-consistent sets) wherein collapse capacities for only a portion of the set are computed with incremental dynamic analysis (IDA) and used as the training data for surrogate modeling. The capacities for the remaining motions, referred to as the test set, are then estimated using the recently introduced data-driven collapse classifier (D2C2) and the automated collapse data constructor (ACDC) technique. These predictions of the collapse capacities of the test set are combined with the training data obtained using IDA to yield the generic collapse fragility of the entire input set of motions. Anti-clustering is used to split the ground motions into the training and test sets to make them as similar as possible to each other while maximizing the difference between ground motions within each set. Scalar intensity measures are used as inputs for the data-driven surrogate. The methodology is tested using steel moment resisting frames ranging from 4 to 20 stories and the FEMA P695 Far Field ground motion set. The results demonstrate the feasibility of the proposed methodology as well as the utility of "small data" machine learning approaches for seismic collapse risk assessments.

Keywords: seismic collapse risk assessment, steel moment resisting frames, small data, data-driven surrogates, ground motion intensity measures

INTRODUCTION

A well-known impediment to the widespread implementation of the performance-based engineering (PBEE) framework [1,2] is the underlying numerical cost associated with the required uncertainty quantification. This aspect is particularly challenging when nonlinear response history analyses are used for collapse risk assessment of both high-fidelity as well as reduced order structural models. In that sense, data-driven machine learning (ML) approaches have been gaining research interest in the earthquake engineering domain [3,4] including efforts to sidestep the nonlinear response history analyses while maintaining their predictive power. For instance, previous research on application of ML tools for seismic fragility assessment revolved around the development of probabilistic seismic demand models and parameterized fragility functions with application to highway bridges e.g. [5–16], single-degree-of-freedom structures on liquefiable sand deposits [17], reinforced concrete (RC) shear walls [18], risk modeling of regional portfolios of structures [12,13,16,18–21] and estimation of the collapse vulnerability of buildings [22–26]. Furthermore, studies [27–29] focused on the use of stochastic surrogate models to better utilize results of linear and nonlinear response history analyses for risk assessments.

Pertinent to this study, Zhong et al. [30] recently studied a surrogate modeling technique called probabilistic learning on manifolds (PLoM) to efficiently estimate the structural responses for systems with variations in design/modeling parameters or ground motion characteristics. At the same time, Bijelić et al. [31] investigated a 'data-centric' approach to ML predictions of collapse risk. Specifically, the authors introduced a surrogate-agnostic data-augmentation approach for seismic collapse capacities termed the automated collapse data constructor (ACDC) technique and the data-driven collapse classifier (D2C2) methodology for collapse prediction. The proposed methodologies were tested for seismic collapse risk estimation of steel

moment resisting frame (MRF) buildings using XGBoost [32] and neural network surrogates, yielding dramatic improvements in the predictive capability compared to baseline cases when not using augmentation even with very small training data.

Building on previous work, this paper focuses on reducing the numerical burden of uncertainty quantification involved in seismic collapse risk assessments with data-driven surrogates as a complement to physics-based response history analyses. Specifically, a methodology is proposed for computing collapse fragilities for generic sets of earthquake records (i.e., not hazard-consistent sets) wherein collapse capacities for only a portion of the set are computed with incremental dynamic analysis (IDA [33]) and used as the training data for surrogate modeling. The capacities for the remaining motions, referred to as the test set, are then estimated using the D2C2 and the ACDC methodologies. These predictions of the collapse capacities of the test set are combined with the training data obtained using IDA to yield the generic collapse fragility of the entire input set of motions. The following sections first briefly recap the ACDC and the D2C2 methodologies and discuss the splitting of the generic ground motion set into the train/test portions using anti-clustering. The proposed approach is then tested in a case study using steel moment resisting frames ranging from 4 to 20 stories and the FEMA P695 [34] Far Field ground motion set. Further refinements of the proposed methodologies, limitations, and the associated research directions are also discussed.

METHODOLOGY

Outline of the approach

The objective of the methodology proposed herein is to reduce the numerical cost associated with estimating the collapse risk of a given structure for a given generic set of earthquake ground motions. As the first step, the ground motion set is split into statistically similar training and testing portions as described in the next section. The IDA analysis is then only performed for the training set to obtain the data used to develop a data-driven surrogate for collapse capacity prediction. In turn, this developed surrogate used to estimate collapse capacities of the ground motions in the test portion. As such, the numerically expensive IDA analysis is not performed for the test set thus affording the reduced cost of the collapse assessment procedure. Specifically, this paper uses equally sized train/test sets as discussed subsequently, hence the numerical cost compared to performing IDAs for the entire generic set is reduced by 50%. Finally, the estimate of the empirical cumulative distribution function (ECDF) of collapse capacities and the associated collapse fragility for the entire set can then be obtained in one of two ways: (a) by merging the predicted collapse capacities obtained using the surrogate on both the training and the test set, or (b) by combining the actual collapse capacities obtained using IDA on the training set with the collapse capacities predicted on the test set using the trained surrogate. We refer to these cases as the "predictions-only" approach and the "mixed" approach, respectively. Both cases are contrasted in the case study presented later in the paper.

In terms of data-driven surrogates, this paper uses the D2C2 methodology [31] to establish the link between the input ground motion and the corresponding collapse response. The D2C2 approach is inspired by the way collapse capacities are computed using numerical response history analyses in the IDA [33] method. Particularly, the response of a structure to a single ground motion is analyzed by amplitude scaling of that ground motion to a set of intensities which are typically represented by the spectral acceleration at the fundamental period of the structure, $S_a(T_1)$. Other intensity measures have been proposed for the same purpose [35,36]. Subsequently, the numerical value of the collapse capacity in IDA procedure is effectively determined by bisection between collapse and non-collapse responses, while the precision to which the collapse capacity is determined is controlled by the choice of intensities at which to perform the response history analysis. In that sense, the collapse response is a binary variable, which allows posing of the collapse capacity prediction as a classification problem, as demonstrated in Figure 1a. Specifically, the grey line indicates the $S_a(T)$ spectra for an example ground motion in the as-recorded (unscaled) format, while the corresponding collapse capacity is indicated with a red dot. The boundary that delineates collapse and non-collapse cases in terms of $S_a(T)$ is obtained by amplitude scaling of the example ground motion to have the value of collapse capacity at $S_a(T_1)$, as indicated by the thick black line. To obtain the data in the classification format, the example ground motion is scaled to several intensities above and below the corresponding collapse capacity. Referring to Figure 1a, the collapse and non-collapse cases are indicated with the dashed and dotted lines, respectively. We refer to this conversion from the regression to the classification format as the data-driven collapse classifier (D2C2) transformation. Given this context, a practical advantage of D2C2 is that it can be directly used in the PBEE framework in the same way that IDA is used, the only difference is that a data-driven surrogate is used instead of a physics-based numerical simulation. For further theoretical and implementation details, the reader is referred to [31].

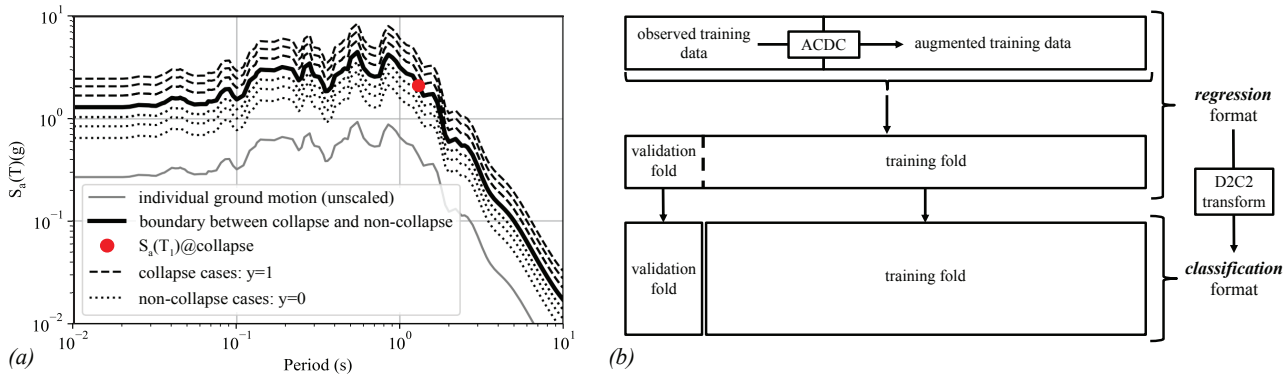

Figure 1. Data preparation flowchart: (a) example of the D2C2 transform from a regression to a classification format for a single ground motion; (b) ACDC augmentation and splitting into cross-validation folds.

Since keeping the data requirements low is practically appealing, the ACDC data augmentation approach is considered in this paper to supplement the small training set with additional synthetic data. The reader is referred to [31] for full details on the ACDC technique, but the main concepts are briefly recapped here. In a nutshell, the ACDC technique leverages the training set data (herein obtained using IDA) to generate statistically similar realizations of the ground motion intensity measures (IMs) and the associated collapse capacities. The ACDC uses the conditional spectrum methodology [37] or its extension, the generalized conditional intensity measure [38] approach, to model the distributions of the ground motions conditioned on the increasing values of the collapse capacities. The weights for the contribution of individual motions from the training set to the conditional intensity measure distributions are obtained using kernel smoothing. Note that no further IDA analyses are required for the ACDC approach. Hence, the numerical cost of the analyses is not increased due to using data augmentation. Additionally, the ACDC approach is model agnostic, i.e., it does not depend on the specific ML or statistical tool that will be trained on the augmented data.

It is also noted that the D2C2 is a surrogate-agnostic methodology, meaning that it can be used with any classification tool. Tuning of the hyperparameters of the selected surrogate is performed using n-fold cross-validation. An important consideration related to data preparation for cross-validation is depicted in Figure 1b. Specifically, the total training data is split into folds while still in the regression format. This ensures that no information from the training fold leaks into the validation fold when the D2C2 transformation to the classification format is performed. In addition, the observed training data and the ACDC augmented data (if used) are treated equally in this paper, meaning that the validation fold is allowed to contain both the real and synthetic data. Finally, given that D2C2 uses a classification approach to obtain the regression estimate of the collapse capacities, both the classification as well as regression metrics can be used for selecting the optimal values of hyperparameters.

Data preparation – ground motion selection using anti-clustering and predictive features

As mentioned previously, the first step of the proposed approach is to split the ground motion set into statistically similar training and testing portions. The rationale for this approach is to ensure that the training data set is similar to the test set thus allowing training of data-driven surrogates that perform well on the test set. To achieve this, the anti-clustering approach [39] is used in this paper. According to [39], the anti-clustering assembles groups in such a way that within-group heterogeneity is high and between-group similarity is high. Thus, anti-clustering reverses the logic of cluster analysis that strives to maximize homogeneity within groups and dissimilarity between groups.

It is important to note that splitting of the ground motion set into two statistically similar portions is performed *a priori*, i.e., before performing any IDA analyses and solely based on the ground motion intensity measures. In this paper, the anti-clustering was performed using the python implementation of the anti-clustering algorithm [39]. In particular, the method maximizing the intra-cluster Euclidean distance between the ground motion IMs was used and partitioning was performed separately for each considered steel MRF. Before partitioning, the ground motions were scaled to have unit value of the spectral acceleration at the fundamental period $S_a(T_1)$. The data was then standardized to have zero-mean and unit variance at each considered IMs. Finally, the ground motions were split into two equally sized sets. As an example, the split of the FEMA P695 [34] ground motion set using anti-clustering for the 4-story MRF is shown in Figure 2. The figure compares the ground motion spectra and a close match between the two sets can be seen both the individual motions (Figure 2a) as well as the conditional spectra (Figure 2b) in the considered period range between $0.2T_1$ and $3.0T_1$ as discussed next.

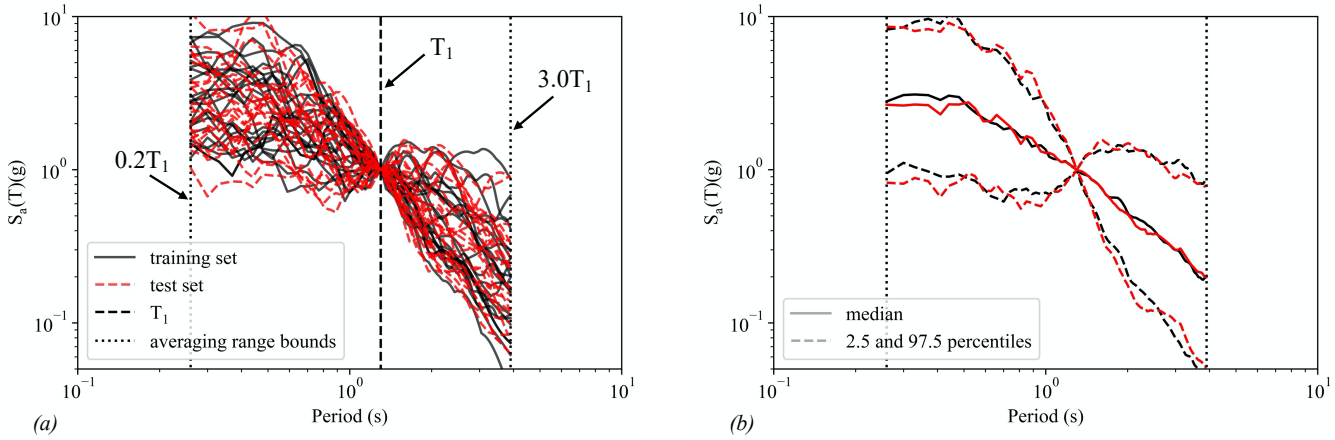

Figure 2. Train and test ground motions sets for the 4-story MRF: (a) individual ground motions, (b) median and 2.5/97.5 percentile spectra.

The vector of IMs used for anti-clustering and, subsequently as predictive features for the data-driven surrogates, consists of scalar IMs extracted from the recorded earthquake waveforms. Specifically, the following IMs are used as input features: (a) spectral accelerations, $S_a(T)$, computed at one hundred periods uniformly spaced between $0.2T_1$ and $3.0T_1$, where T_1 is the fundamental period of the steel MRF for which the ground motions are used (Note: if $3.0T_1$ is larger than 10s, then the period of 10s is used as the upper bound; this limit is imposed primarily due to lack of ground motion prediction equations for predicting spectral values at periods longer than 10s amongst other constraints [40]); (b) the average spectral acceleration, $S_{a,avg}(0.2\ T_1 - 3.0\ T_1)$ [41]; (c) $S_{a,ratio}$ which is defined as $S_a(T_1)/S_{a,avg}$ [41]; (d) the 5-75% and the 5-95% significant durations, $D_{a,5-75\%}$ and $D_{a,5-95\%}$ [42] respectively; (e) the filtered incremental velocity, $FIV3$ [43]; and (f) the ratio of $FIV3$ and $S_{a,avg}$ which we termed as $\text{FIV3}_{a,ratio}$ [31]. Hence, the feature vector has 106 elements each corresponding to one of the scalar IMs that are used as predictive features. The rationale for choosing these IMs is that, to the extent of current earthquake engineering knowledge, they collectively represent a simplified, yet comprehensive description of the ground motion parameters that correlate well with structural response and particularly for collapse response of MRFs as investigated herein.

CASE-STUDY APPLICATION TO STEEL MOMENT RESISTING FRAMES

Case study buildings and ground motions

A 4-, 8-, 12-, and a 20-story steel MRF buildings designed by Skiadopoulos and Lignos [44] are used in this paper. The response spectrum analysis procedure is employed as the basis for the design of these frames. Welded unreinforced flange-welded web (WUF-W) beam-to-column connections are employed. The steel buildings are located in urban California (seismic design category: $SDC = D_{max}$; soil class D). Two-dimensional (2D) nonlinear models of the steel MRFs are developed in the open-source simulation platform OpenSees [45], see Figure 3. The 2D models are idealized based on the concentrated plasticity approach. Rotational springs, located at the plastic hinge regions, are used to model the nonlinear behavior of the columns and beams. These springs utilize the modified IMK model deterioration model [46–48] that can capture the cyclic deterioration in flexural strength and stiffness of steel components subjected to cyclic loading. The panel zone is modeled using the parallelogram model proposed by Gupta and Krawinkler [49] where the hysteretic behavior of the panel zone is bounded by a tri-linear backbone curve proposed by Skiadopoulos et al. [50]. P-Delta effects are considered by using a fictitious column (noted as the 'leaning column') connected to the steel MRF by axially rigid truss elements. The leaning column is loaded at each floor with a vertical load equal to half of the seismic gravity load of the building minus the tributary load that is directly assigned to the MRF columns. The contribution of the gravity framing to the lateral strength and stiffness of the steel MRFs is not considered in the present study. Rayleigh damping is incorporated in the 2D models as discussed by Zareian and Medina [51]. Two percent damping ratio (ζ = 2%) is assumed at the first mode (T_1) and one fifth of T_1 of the steel MRFs. The fundamental periods equal $1.3s$, $2.1s$, $2.5s$ and $4.0s$ for the 4-story to 20-story steel MRFs, respectively (see [44]).

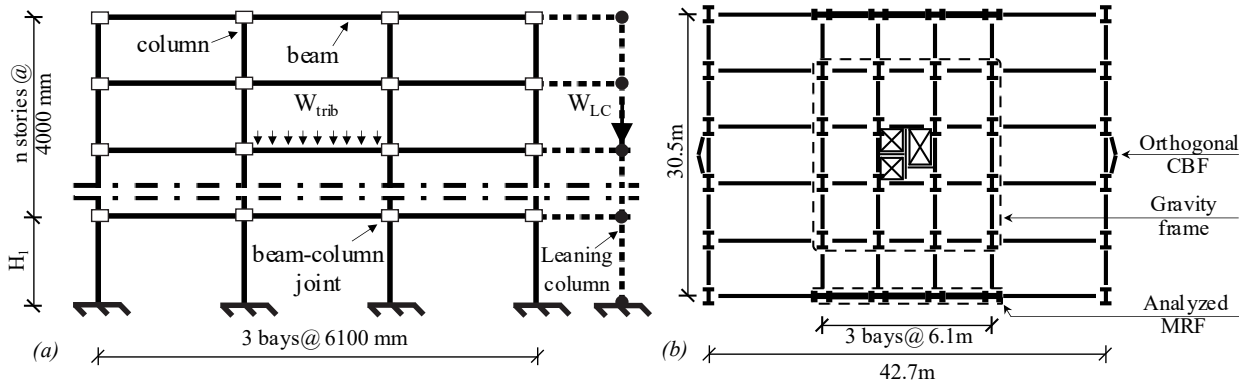

Figure 3. Scheme of the 2D structural models for the 4-, 8-, 12-, and 20-story steel moment resisting frames: (a) elevation; (b) plan (adapted from [44]). The first story height (H_1) is 4300 mm for the 4-story frame and 4200 mm for other frames.

The FEMA P-695 [34] Far-Field set of 44 short duration ground motion seismograms is used to conduct the collapse risk assessment. This generic set of ground motions (i.e., not hazard-consistent with any specific site) is the de facto standard for quantifying the uncertainty of ground shaking in collapse assessments. The anti-clustering approach described previously is used to split the entire set into the training and testing portions each containing 22 motions (e.g., see Figure 1). The training and test sets are specific to each of the considered MRFs. To keep data requirements as low as possible, there is no separate validation set used herein. Rather, n-fold cross-validation is used for hyperparameter tuning as described in the next section.

Case study D2C2 surrogates

This paper uses boosted regression tree classifier, specifically the XGBoost [32], as the underlying surrogate of the D2C2 methodology. The following hyperparameters are tuned using the 4-fold cross-validation: `max_depth`, `eta`, `subsample`, `colsample_bytree`, and `alpha`. All parameters are tuned concurrently. A detailed description of XGBoost including definitions of hyperparameters is available in the online documentation [52] but a brief explanation is provided herein. The `max_depth` parameter controls the maximum number of nodes each boosted tree can have, where a larger value indicates a more complex surrogate that is more likely to overfit. The `subsample` and the `colsample_bytree` parameters are used to control overfitting and indicate the proportion of the training samples and features to be used while growing the trees, respectively. Setting their values to unity means that all the samples and all features are used, implying no regularization from feature or sample selection during the training process. At the same time, `alpha` is the cost used to impose L1 regularization. Finally, `eta` is the learning rate of the algorithm. The optimal values of the hyperparameters in this paper are selected based on the mean absolute percentage error (MAPE [53]) metric obtained in 150 boosting rounds. Note that MAPE is a regression metric, and it is possible to use it herein because in D2C2 the classification approach is used to obtain the regression estimate of the collapse capacities. All other hyperparameters are set to default values as used in the python implementation of XGBoost (version 1.3.3). Binary logistic loss [54] is used as the objective function. When training the final data-driven models with the tuned hyperparameters, randomly chosen 20% of the real training data is used as a validation set to initiate early stopping based on the validation loss. The final models are then trained using entire considered training data for the optimal number of boosting rounds (i.e., the number of rounds when early stopping was initiated).

The optimal values of the hyperparameters obtained using cross-validation are summarized in Table 1. The surrogates are tuned for all MRFs considering the cases both with and without ACDC augmentation. A general observation is that the optimal values of the `colsample_bytree` and `subsample` parameters are in all cases less than one. This means that the surrogates are regularized both by not considering all the predictive features (IMs) as well as by not considering all of the available training samples when building the regression trees. Dropping some of the IMs from the final surrogates is sensible from the structural dynamics viewpoint as the considered MRFs are not equally sensitive to all considered features. On the other hand, not including all of the samples when building the trees (i.e., `subsample` < 1.0) could potentially indicate that some of the samples in certain cases introduce biases in the predictions which may be stemming from the use of IMs as predictive features. For instance, meaningfully different structural responses to ground motions that have similar IMs are possible (e.g., due to the "resurrection" effect) since the IMs are simplified proxies for complex ground motion waveforms. This is a challenge particularly when using small training sets and is left for subsequent studies.

Table 1. Tuned values of the xgboost surrogate hyperparameters used in D2C2.

MRF	ACDC	Hyperparameters				
		max_depth	eta	subsample	colsample_bytree	alpha
4-story	no	1	0.005440	0.634582	0.610919	0.005260
	yes	1	0.083407	0.642931	0.579314	0.002000
8-story	no	1	0.671676	0.844104	0.723093	0.002000
	yes	1	0.345484	0.818220	0.510067	0.002000
12-story	no	1	0.202817	0.451382	0.300547	0.002000
	yes	1	0.192804	0.494132	0.453166	0.002000
20-story	no	1	0.817902	0.621440	0.537083	0.002000
	yes	3	0.581816	0.559729	0.654705	0.002000

In terms of surrogate model complexity, the optimal value of the `max_depth` parameter equals unity in almost all considered cases (see Table 1). Specifically, only the 20-story MRF trained with ACDC benefitted from a more complex model (`max_depth` = 3). Finally, when tuning the 4-story MRF it was noticed that `alpha` parameter did not have a strong effect on the predictive performance of the surrogate. Hence, the value of `alpha` was kept fixed at 0.002 during tuning for the remaining cases. The D2C2 surrogates trained with these tuned hyperparameter values were used to obtain the results presented in the following section. These hyperparameter values could also be used as starting points in subsequent research studies.

Collapse risk assessment results

The developed D2C2 surrogates are used to make collapse predictions for the considered MRFs. Shown in Figure 4 are the results for the 8-story MRF. Referring to Figure 4a, plotted with a black line is the ECDF of the collapse capacities obtained using IDA for the 44 ground motions of the FEMA P695 ground motion set. We refer to this data as the "true data" to differentiate it from the estimates obtained using surrogates, i.e., the results of the nonlinear response history analyses are considered the ground truth for the purpose of this study. Indicated with the grey dotted line in the same figure is the ECDF of the collapse capacities of the 22 ground motions, which were used as the training set for the development of the data-driven surrogates. Note that the ECDFs of the training data and the true data are not matching closely. In other words, a collapse fragility simply fitted to the training data will not closely represent the fragility fitted to the true data, as shown in Figure 4b. In particular, the fragility fitted to the training data in this case underestimates the median collapse capacity, θ_{col}, for about 7% (0.63g compared to 0.68g, respectively) and the dispersion, β_{col}, for about 8% (0.35 compared to 0.38) relative to the fragility fitted to the true data.

In contrast, using the D2C2 surrogate can yield improved predictions. Still referring to Figures 4a and 4b, the median collapse capacity estimates obtained using the D2C2 surrogate (indicated with the gray line with cross-shaped markers) is in closer agreement with the true data. Specifically, the difference of θ_{col} is on the order of 4% (0.66g compared to 0.68g). However, the difference in the estimates of β_{col} significantly increased to about 23%, which can also be seen in a relatively poor match between ECDFs. If, however, the ACDC augmented data is used in addition to the real training data then the D2C2 surrogate yields predictions that are in close agreement with the true data, as seen from the red dashed lines in the Figure 4. In this case, the difference in θ_{col} and β_{col} is 1.7% and 0.9% compared to the true data. For comparison purposes, the collapse estimates obtained using the hazard-consistent IDA (HC-IDA [55]) approach are also shown in the same figure. HC-IDA is a reliability-based method, which leverages a linear regression surrogate fitted to the collapse data to obtain a non-parametric estimate of the collapse fragility through integration with the hazard data [56]. In that sense, shown with a blue line with circular markers in Figure 4a are the mean estimates obtained for each ground motion using the linear surrogate from HC-IDA while the Figure 4b shows the collapse fragility obtained after integration with the hazard data. This is an important difference to the D2C2 approach, as the HC-IDA fragility in Figure 4b is not simply obtained by fitting a log-normal distribution to the ECDF data in Figure 4a. As seen from the graph, in this case the HC-IDA fragility is in close agreement to the true data with the differences of 1.7% and 5.7% for θ_{col} and β_{col}, respectively.

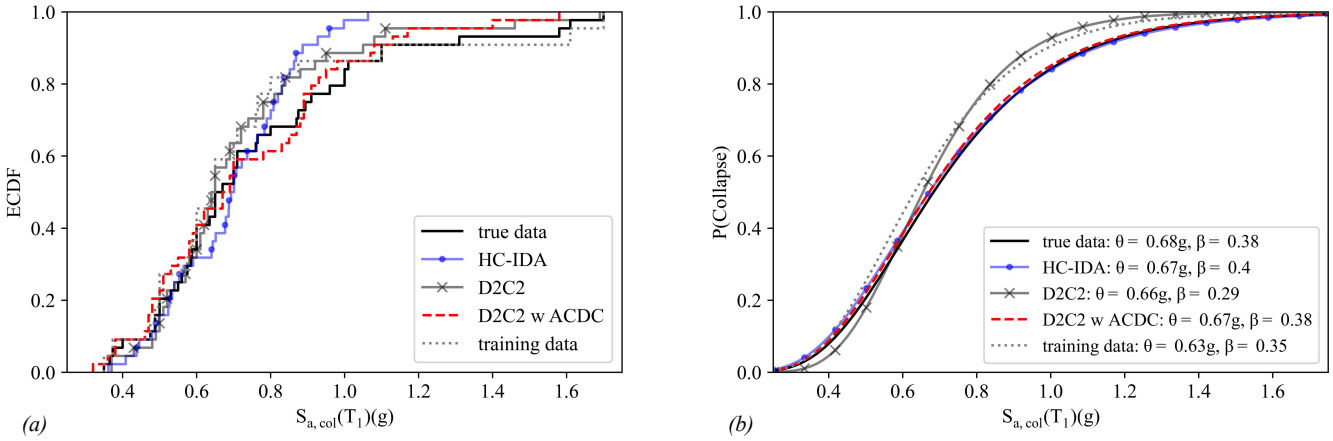

Figure 4. Collapse capacity and fragility estimates for the 8-story MRF: (a) ECDFs and (b) collapse fragilities obtained using the "predictions-only" approach.

These estimates of the collapse fragilities of the 8-story MRF are summarized in Table 2. Also shown in the table are the mean annual frequencies of collapse, λ^* and λ, obtained by integration of the $S_a(T_1)$ hazard curve at the design location with both the ECDFs and the collapse fragilities, respectively. The results are provided for the "prediction-only" approach (as shown in Figure 4) and the "mixed" approach (shown in Figure 5). The difference between the two approaches is that the "prediction-only" approach uses predicted collapse capacities for the entire ground motion set while the "mixed" approach uses predictions only on the test set and the true values from the training set. This can be seen from the scatterplots in Figures 5a and 5b, where the true values of the collapse capacities are compared to the values obtained using the surrogates. Referring to Figure 5a, the values of collapse capacities of the training data (i.e., the observed set indicated with black dots) when using the "predictions-only" approach are distributed around the dashed black line with a unit slope going through the origin. In contrast, when using the "mixed" approach, these points lie along the dashed black line. The corresponding difference in the resulting ECDFs and collapse fragilities is shown in Figures 5c and 5d. As a general observation, both approaches seem viable in terms of estimating λ. For instance, the difference from the true data in terms of the mean annual frequency of collapse obtained with the D2C2 trained using the ACDC is on the order of 4.5% and 2.4% for the predictions-only and the mixed approaches, respectively. This stems from a close match in the *lower tails* of the collapse fragilities, as seen by comparing the full black line and the dashed red lines in Figures 4b and 5d. However, the *entire* collapse fragility from the "predictions-only" approach is in closer agreement with the true fragility compared to the "mixed" approach case.

Table 2. Collapse risk estimates, 8-story steel MRF.

8-story MRF		λ^* [10^{-4}]	difference [%]	θ_{col}(g)	diff. [%]	β_{col}	diff. [%]	λ [10^{-4}]	diff. [%]
	true data	5.3242	/	0.684	/	0.380	/	5.9803	/
prediction only approach	HC-IDA	5.1275	-3.70	0.672	-1.66	0.401	5.74	6.4244	7.43
	D2C2	5.3392	0.28	0.655	-4.16	0.291	-23.29	5.7933	-3.13
	D2C2 w ACDC	5.6708	6.51	0.672	-1.72	0.383	0.86	6.2447	4.42
mixed approach	D2C2	5.5338	3.94	0.651	-4.72	0.304	-19.91	5.9687	-0.20
	D2C2 w ACDC	5.5940	5.07	0.664	-2.86	0.353	-6.96	6.1229	2.38

Note: λ^* and λ are obtained by integration of the ECDF and the collapse fragility with the hazard curve, respectively.

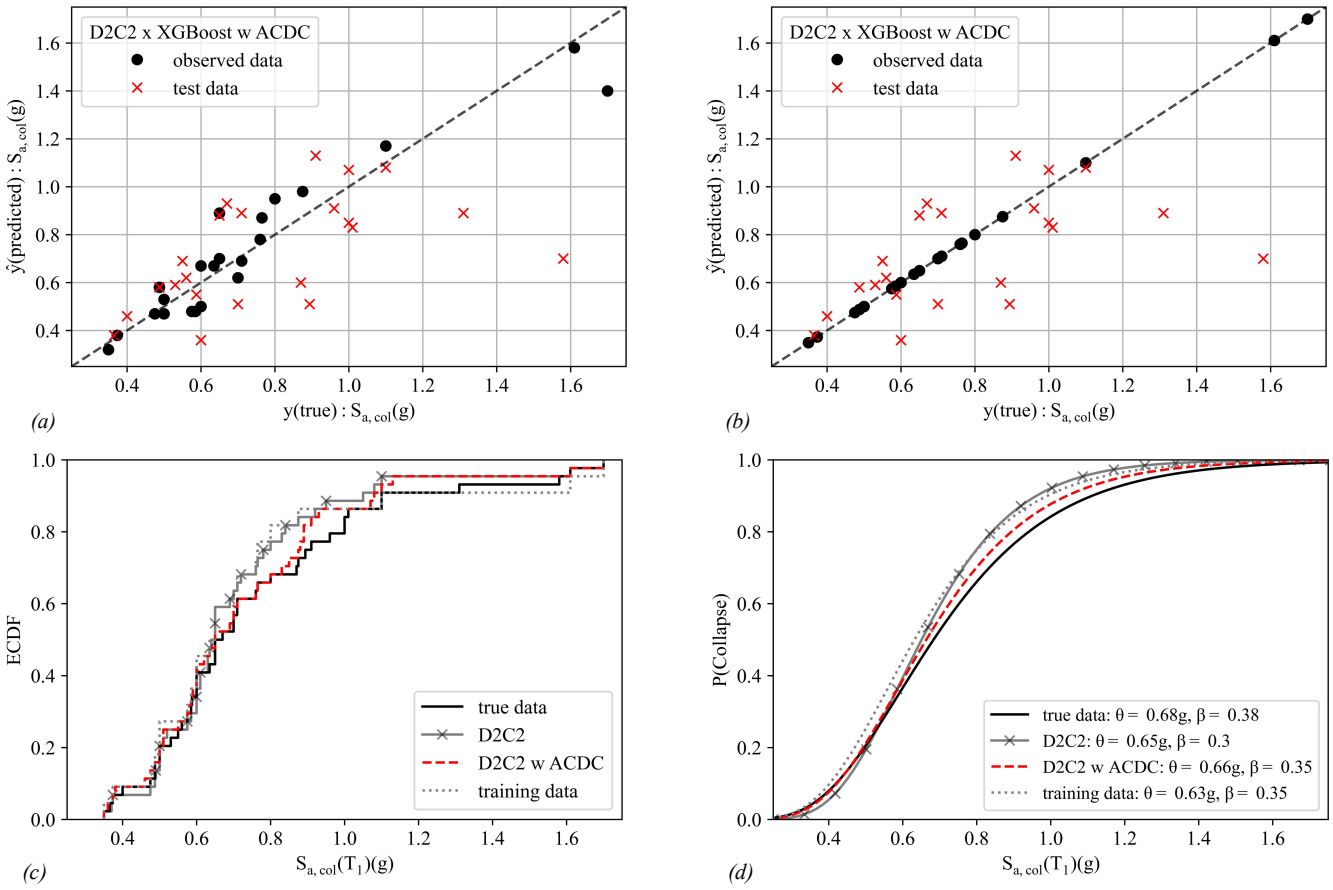

Figure 5. True vs predicted collapse capacities, 8-story MRF: (a) "predictions-only" approach; (b) "mixed" approach; (c) and (d) ECDFs and collapse fragilities obtained using the "mixed" approach.

A general observation from all the steel MRFs analyzed in this study is that the "mixed" approach using D2C2 with ACDC yields collapse fragilities that are either in a less good or an as good of an agreement with the true data compared to the corresponding "predictions-only" approach. In other words, the results of this study slightly favor the "predictions-only" approach compared to the "mixed" approach, but research results from additional frames are needed for definitive statements. Furthermore, the observations related to the D2C2 surrogates presented for the 8-story MRF qualitatively hold for all considered steel frames. To streamline the presentation, Figure 6 and Table 3 show the results for the 20-story MRF while the results for the 4-story and the 12-story MRFs are provided in Tables 4 and 5, respectively. Referring to the Figure 6a, the ECDF estimated using the D2C2 surrogate trained with ACDC data (red dashed line) is in very close agreement with the true data ECDF (black full line) save for the region around the 80-th to 90-th percentile. In turn, this translates into closely matching fragility curves (Figure 6b) which do have a difference in the upper tail. This difference is driven by the ~7% overestimation of the β_{col} (0.37 compared to 0.34) and about 2.6% overestimation of the θ_{col} (0.35g compared to 0.34g) as given in Table 3. At the same time, the error of λ estimated using the D2C2 surrogate trained with ACDC is on the order of 2%. This is in stark contrast to the HC-IDA predictions, indicated with a blue line with circular markers in Figure 6b, yielding about 12% error in λ which stems from about 24% overestimation of β_{col} (0.43 compared to true value of 0.34). All off the surrogates used on the 20-story frame yield errors in the median collapse capacities, θ_{col}, that are less than 5%.

While not shown in the figures, the HC-IDA fragilities for the 4- and 12-story MRFs have a similar predictive error with that of the 20-story case (i.e., close agreement with the true data was only observed in the case of the 8-story MRF as shown in Figure 8b). It should be noted here that the HC-IDA method uses only two predictors ($S_{a,ratio}$and $D_{a,5\text{-}75\%}$ significant duration) compared to the 106 predictors used in the D2C2. In addition, the HC-IDA as used herein is based on a global (i.e., fitted to all data) linear regression surrogate which makes it less flexible compared to the XGBoost surrogate used for D2C2. For these reasons, ACDC is not considered when using HC-IDA in this paper. However, combining local regression in HC-IDA (as proposed in [56]) with the ACDC augmentation could be considered in follow-up studies given practical ease of implementing HC-IDA as any required hyperparameter tuning would be expedient.

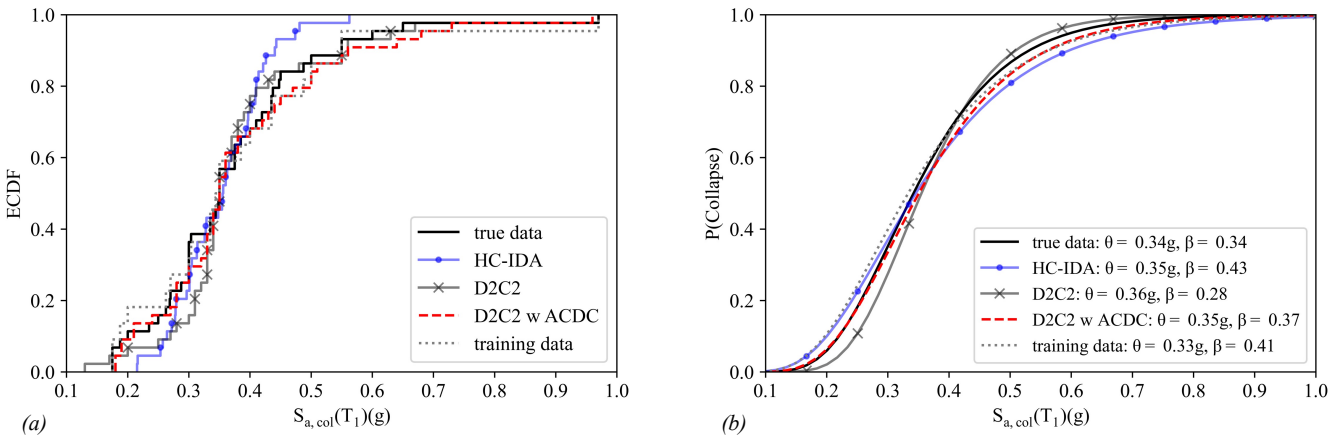

Figure 6. Collapse response estimates for the 20-story MRF obtained using the "predictions-only" approach: (a) ECDFs; (b) collapse fragilities.

Table 3. Collapse risk estimates, 20-story MRF.

20-story MRF		λ^* [10^{-4}]	difference [%]	θ_{col}(g)	diff. [%]	β_{col}	diff. [%]	λ [10^{-4}]	diff. [%]
	true data	4.3268	/	0.342	/	0.343	/	4.5192	/
prediction only approach	HC-IDA	3.5949	-16.92	0.346	1.08	0.426	23.95	5.0729	12.25
	D2C2	3.9084	-9.67	0.355	3.80	0.281	-18.18	3.7674	-16.63
	D2C2 w ACDC	4.1087	-5.04	0.351	2.56	0.367	6.76	4.4271	-2.04
mixed approach	D2C2	3.9942	-7.69	0.352	2.91	0.334	-2.82	4.1623	-7.90
	D2C2 w ACDC	4.2261	-2.33	0.348	1.83	0.372	8.27	4.5404	0.47

Note: λ^* and λ are obtained by integration of the ECDF and the collapse fragility with the hazard curve, respectively.

Table 4. Collapse risk estimates, 4-story MRF.

4-story MRF		λ^* [10^{-4}]	difference [%]	θ_{col}(g)	diff. [%]	β_{col}	diff. [%]	λ [10^{-4}]	diff. [%]
	true data	5.2313	/	1.214	/	0.455	/	5.8371	/
prediction only approach	HC-IDA	3.9337	-24.81	1.269	4.58	0.382	-16.21	4.5379	-22.26
	D2C2	4.6129	-11.82	1.229	1.22	0.411	-9.83	5.1890	-11.10
	D2C2 w ACDC	4.7975	-8.29	1.213	-0.10	0.430	-5.56	5.5592	-4.76
mixed approach	D2C2	4.5939	-12.19	1.242	2.34	0.411	-9.65	5.0643	-13.24
	D2C2 w ACDC	4.6917	-10.31	1.234	1.71	0.430	-5.56	5.3313	-8.66

Note: λ^* and λ are obtained by integration of the ECDF and the collapse fragility with the hazard curve, respectively.

Table 5. Collapse risk estimates, 12-story MRF.

12-story MRF		λ^* [10^{-4}]	difference [%]	θ_{col}(g)	diff. [%]	β_{col}	diff. [%]	λ [10^{-4}]	diff. [%]
	true data	3.5435	/	0.707	/	0.396	/	3.6774	/
prediction only approach	HC-IDA	3.1365	-11.49	0.662	-6.31	0.367	-7.26	4.0657	10.56
	D2C2	3.2446	-8.44	0.697	-1.44	0.320	-19.07	3.3332	-9.36
	D2C2 w ACDC	3.3598	-5.18	0.700	-1.02	0.379	-4.21	3.6519	-0.69
mixed approach	D2C2	3.4144	-3.64	0.693	-1.94	0.348	-12.21	3.5303	-4.00
	D2C2 w ACDC	3.4708	-2.05	0.697	-1.37	0.389	-1.88	3.7457	1.86

Note: λ^* and λ are obtained by integration of the ECDF and the collapse fragility with the hazard curve, respectively.

CONCLUSIONS

This paper proposed a methodology, which combines explicit nonlinear response history analyses with physical model representations of steel frame buildings and data-driven surrogates for collapse risk assessment using generic ground motion sets. The method reduces the computational expense required for the underlying uncertainty quantification by leveraging anti-clustering to split the ground motions into statistically similar and equally sized training and test sets. The data-driven collapse classifier (D2C2) methodology and the automated collapse data constructor (ACDC) techniques are then utilized on a training set to develop a data-driven surrogate, which is applied to estimate the collapse capacities on the test portion of the data and yield the combined result for the entire generic ground motion set. Since the numerically expensive collapse capacity estimation using IDA is only performed on the training set, the methodology reduces the computational cost by 50%. The methodology was tested using the FEMA P695 Far Field ground motion set and a set of steel MRFs ranging in height from 4- to 20-stories.

The main contribution and observation of this paper is that the proposed methodology allows for the development of data-driven surrogates with predictive power that rivals the full physics-based IDA, but at a considerably reduced computational expense. For example, the errors in the mean annual frequencies of collapse (λ) obtained using the proposed methodology were smaller than 5% compared to the ground truth (full IDA) for all considered MRFs in the performed case-study. Specifically, the errors in λ range from 0.7% to 4.7%. Moreover, the methodology allows estimation of the entire collapse fragilities, and not just the lower tails, that are in close agreement with the ground truth. For the considered MRFs, the errors in the median collapse capacities (θ_{col}) range from 0.1% to 2.5%, while the errors in dispersions (β_{col}) are on the order of 0.9% to 6.8%. Note that in all cases, the data-driven surrogates were trained using only 22 data points. As such, these are very promising results that demonstrate the feasibility of the proposed methodology as well as the utility of "small data" machine learning approaches for seismic collapse risk assessments of capacity-designed frame buildings.

ACKNOWLEDGMENTS

This research was sponsored by the Swiss National Science Foundation (FNS Spark Award Number: CRSK-2_190535) and additional funding provided by an EPFL internal grant. This financial support is greatly appreciated. The first author thanks Prof. Baker, Prof. Deierlein, Prof. Chandramohan, and Prof. Zhong for developing the insightful and inspiring HC-IDA and SAF-IDA methods. Any opinions, findings, and conclusions or recommendations expressed in this paper are those of the authors and do not necessarily reflect the views of sponsors.

REFERENCES

[1] Applied Technology Council (ATC), Earthquake Damage Evaluation Data for California. Report ATC-13., Redwood City, CA, USA, 1985.

[2] J.P. Moehle, A framework for performance-based earthquake engineering., in: Proceedings of 10th U.S. - Japan Workshop on the Improvement of Building Structural Design and Construction Practices, Report ATC-15-9, Maui, HI, 2003.

[3] Y. Xie, M. Ebad Sichani, J.E. Padgett, R. DesRoches, The promise of implementing machine learning in earthquake engineering: A state-of-the-art review, Earthquake Spectra. 36 (2020) 1769–1801. https://doi.org/10.1177/8755293020919419.

[4] G.G. Deierlein, Adam Zsarnóczay, eds., State of the Art in Computational Simulation for Natural Hazards Engineering, Zenodo, 2021. https://doi.org/10.5281/ZENODO.4558106.

[5] Y. Xie, Q. Zheng, C.-S.W. Yang, W. Zhang, R. DesRoches, J.E. Padgett, E. Taciroglu, Probabilistic models of abutment backfills for regional seismic assessment of highway bridges in California, Engineering Structures. 180 (2019) 452–467. https://doi.org/10.1016/j.engstruct.2018.11.058.

[6] Y. Xie, J. Zhang, Optimal Design of Seismic Protective Devices for Highway Bridges Using Performance-Based Methodology and Multiobjective Genetic Optimization, Journal of Bridge Engineering. 22 (2017) 04016129 1–13. https://doi.org/10.1061/(ASCE)BE.1943-5592.0001009.

[7] Y. Xie, J. Zhang, Design and Optimization of Seismic Isolation and Damping Devices for Highway Bridges Based on Probabilistic Repair Cost Ratio, Journal of Structural Engineering. 144 (2018) 04018125 1–13. https://doi.org/10.1061/(ASCE)ST.1943-541X.0002139.

[8] J. Dukes, S. Mangalathu, J.E. Padgett, R. DesRoches, Development of a bridge-specific fragility methodology to improve the seismic resilience of bridges, Earthquakes and Structures. 15 (2018) 253–261. https://doi.org/10.12989/eas.2018.15.3.253.

[9] J. Ghosh, J.E. Padgett, L. Dueñas-Osorio, Surrogate modeling and failure surface visualization for efficient seismic vulnerability assessment of highway bridges, Probabilistic Engineering Mechanics. 34 (2013) 189–199. https://doi.org/10.1016/j.probengmech.2013.09.003.

[10] J. Ghosh, K. Rokneddin, J.E. Padgett, L. Dueñas-Osorio, Seismic Reliability Assessment of Aging Highway Bridge Networks with Field Instrumentation Data and Correlated Failures, I: Methodology, Earthquake Spectra. 30 (2014) 795–817. https://doi.org/10.1193/040512EQS155M.

[11] J. Ghosh, P. Sood, Consideration of time-evolving capacity distributions and improved degradation models for seismic fragility assessment of aging highway bridges, Reliability Engineering & System Safety. 154 (2016) 197–218. https://doi.org/10.1016/j.ress.2016.06.001.

[12] J.-S. Jeon, S. Mangalathu, J. Song, R. Desroches, Parameterized Seismic Fragility Curves for Curved Multi-frame Concrete Box-Girder Bridges Using Bayesian Parameter Estimation, Journal of Earthquake Engineering. 23 (2019) 954–979. https://doi.org/10.1080/13632469.2017.1342291.

[13] S. Kameshwar, J.E. Padgett, Multi-hazard risk assessment of highway bridges subjected to earthquake and hurricane hazards, Engineering Structures. 78 (2014) 154–166. https://doi.org/10.1016/j.engstruct.2014.05.016.

[14] S. Kameshwar, J.E. Padgett, Effect of vehicle bridge interaction on seismic response and fragility of bridges, Earthquake Engineering & Structural Dynamics. 47 (2018) 697–713. https://doi.org/10.1002/eqe.2986.

[15] S. Mangalathu, J.-S. Jeon, R. DesRoches, Critical uncertainty parameters influencing seismic performance of bridges using Lasso regression, Earthquake Engineering & Structural Dynamics. 47 (2018) 784–801. https://doi.org/10.1002/eqe.2991.

[16] S. Mangalathu, G. Heo, J.-S. Jeon, Artificial neural network based multi-dimensional fragility development of skewed concrete bridge classes, Engineering Structures. 162 (2018) 166–176. https://doi.org/10.1016/j.engstruct.2018.01.053.

[17] P.S. Koutsourelakis, Assessing structural vulnerability against earthquakes using multi-dimensional fragility surfaces: A Bayesian framework, Probabilistic Engineering Mechanics. 25 (2010) 49–60. https://doi.org/10.1016/j.probengmech.2009.05.005.

[18] A.J. Yazdi, T. Haukaas, T. Yang, P. Gardoni, Multivariate Fragility Models for Earthquake Engineering, Earthquake Spectra. 32 (2016) 441–461. https://doi.org/10.1193/061314EQS085M.

[19] M. Ebad Sichani, J.E. Padgett, V. Bisadi, Probabilistic seismic analysis of concrete dry cask structures, Structural Safety. 73 (2018) 87–98. https://doi.org/10.1016/j.strusafe.2018.03.001.

[20] Y. Xie, J. Zhang, R. DesRoches, J.E. Padgett, Seismic fragilities of single-column highway bridges with rocking column-footing, Earthquake Engineering & Structural Dynamics. 48 (2019) 843–864. https://doi.org/10.1002/eqe.3164.

[21] J. Zhang, Y. Xie, G. Wu, Seismic responses of bridges with rocking column-foundation: A dimensionless regression analysis, Earthquake Engineering & Structural Dynamics. 48 (2019) 152–170. https://doi.org/10.1002/eqe.3129.

[22] N. Bijelić, T. Lin, G. Deierlein, Classification algorithms for collapse prediction of tall buildings and regional risk estimation utilizing SCEC CyberShake simulations, in: Proceedings of the 13th International Conference on Applications of Statistics and Probability in Civil Engineering, Seoul, South Korea, 2019. https://doi.org/10.22725/ICASP13.111.

[23] H.V. Burton, S. Sreekumar, M. Sharma, H. Sun, Estimating aftershock collapse vulnerability using mainshock intensity, structural response and physical damage indicators, Structural Safety. 68 (2017) 85–96. https://doi.org/10.1016/j.strusafe.2017.05.009.

[24] N. Bijelić, T. Lin, G.G. Deierlein, Efficient intensity measures and machine learning algorithms for collapse prediction of tall buildings informed by SCEC CyberShake ground motion simulations, Earthquake Spectra. 36 (2020) 1188–1207. https://doi.org/10.1177/8755293020919414.

[25] S.-H. Hwang, S. Mangalathu, J. Shin, J.-S. Jeon, Machine learning-based approaches for seismic demand and collapse of ductile reinforced concrete building frames, Journal of Building Engineering. 34 (2021) 101905. https://doi.org/10.1016/j.jobe.2020.101905.

[26] F. Pourkamali-Anaraki, M.A. Hariri-Ardebili, Neural Networks and Imbalanced Learning for Data-Driven Scientific Computing With Uncertainties, IEEE Access. 9 (2021) 15334–15350. https://doi.org/10.1109/ACCESS.2021.3052680.

[27] B. Sudret, C.V. Mai, Computing seismic fragility curves using polynomial chaos expansions, in: Eidgenössische Technische Hochschule Zürich, 2013. https://doi.org/10.3929/ethz-a-010060735.

[28] X. Zhu, M. Broccardo, B. Sudret, Seismic fragility analysis using stochastic polynomial chaos expansions, (2022). https://doi.org/10.48550/arXiv.2208.07747.

[29] A.P. Kyprioti, A.A. Taflanidis, Kriging metamodeling for seismic response distribution estimation, Earthquake Engineering & Structural Dynamics. 50 (2021) 3550–3576. https://doi.org/10.1002/eqe.3522.

[30] K. Zhong, J.G. Navarro, S. Govindjee, G.G. Deierlein, Surrogate modeling of structural seismic response using probabilistic learning on manifolds, Earthquake Engineering & Structural Dynamics. n/a (n.d.). https://doi.org/10.1002/eqe.3839.

[31] N. Bijelić, D.G. Lignos, A. Alahi, The Data-Driven Collapse Classifier (D2C2) methodology and the Automated Collapse Data Constructor (AC/DC) technique for robust seismic collapse fragility and risk estimation – effective training of surrogate models with 'small data' by leveraging domain-specific data augmentation and hyperparameter tuning., Earthquake Engineering & Structural Dynamics (Final Draft Ready, Submission Expected in February 2022). (-).

[32] T. Chen, C. Guestrin, XGBoost: A Scalable Tree Boosting System, Proceedings of the 22nd ACM SIGKDD International Conference on Knowledge Discovery and Data Mining. (2016) 785–794. https://doi.org/10.1145/2939672.2939785.

[33] D. Vamvatsikos, C.A. Cornell, Incremental dynamic analysis, Earthquake Engng. Struct. Dyn. 31 (2002) 491–514. https://doi.org/10.1002/eqe.141.
[34] Federal Emergency Management Agency (FEMA), Quantification of building seismic performance factors. tech. rep., FEMA P-695, Washington, D.C., 2009.
[35] D. Vamvatsikos, C.A. Cornell, Developing efficient scalar and vector intensity measures for IDA capacity estimation by incorporating elastic spectral shape information, Earthquake Engineering & Structural Dynamics. 34 (2005) 1573–1600. https://doi.org/10.1002/eqe.496.
[36] A.K. Kazantzi, D. Vamvatsikos, Intensity measure selection for vulnerability studies of building classes, Earthquake Engineering & Structural Dynamics. 44 (2015) 2677–2694. https://doi.org/10.1002/eqe.2603.
[37] J. Baker, Conditional Mean Spectrum: Tool for Ground-Motion Selection, Journal of Structural Engineering. 137 (2011) 322–331. https://doi.org/10.1061/(ASCE)ST.1943-541X.0000215.
[38] B.A. Bradley, A generalized conditional intensity measure approach and holistic ground-motion selection, Earthquake Engineering & Structural Dynamics. 39 (2010) 1321–1342. https://doi.org/10.1002/eqe.995.
[39] M. Papenberg, G.W. Klau, Using anticlustering to partition data sets into equivalent parts, (2019). https://doi.org/10.31234/osf.io/3razc.
[40] L. Eads, Seismic collapse risk assessment of buildings: Effects of intensity measure selection and computational approach, Stanford University, 2013.
[41] L. Eads, E. Miranda, D. Lignos, Spectral shape metrics and structural collapse potential, Earthquake Engng Struct. Dyn. 45 (2016) 1643–1659. https://doi.org/10.1002/eqe.2739.
[42] J.J. Kempton, J.P. Stewart, Prediction Equations for Significant Duration of Earthquake Ground Motions Considering Site and Near-Source Effects, Earthquake Spectra. 22 (2006) 985–1013. https://doi.org/10.1193/1.2358175.
[43] H. Dávalos, E. Miranda, Filtered incremental velocity: A novel approach in intensity measures for seismic collapse estimation, Earthquake Engineering & Structural Dynamics. 48 (2019) 1384–1405. https://doi.org/10.1002/eqe.3205.
[44] A. Skiadopoulos, D.G. Lignos, Seismic demands of steel moment resisting frames with inelastic beam-to-column web panel zones, Earthquake Engineering & Structural Dynamics. 51 (2022) 1591–1609. https://doi.org/10.1002/eqe.3629.
[45] F. McKenna, M.H. Scott, G.L. Fenves, Nonlinear Finite-Element Analysis Software Architecture Using Object Composition, Journal of Computing in Civil Engineering. 24 (2010) 95–107. https://doi.org/10.1061/(ASCE)CP.1943-5487.0000002.
[46] L.F. Ibarra, R.A. Medina, H. Krawinkler, Hysteretic models that incorporate strength and stiffness deterioration, Earthquake Engineering & Structural Dynamics. 34 (2005) 1489–1511. https://doi.org/10.1002/eqe.495.
[47] D.G. Lignos, A.R. Hartloper, A. Elkady, G.G. Deierlein, R. Hamburger, Proposed Updates to the ASCE 41 Nonlinear Modeling Parameters for Wide-Flange Steel Columns in Support of Performance-Based Seismic Engineering, Journal of Structural Engineering. 145 (2019) 04019083. https://doi.org/10.1061/(ASCE)ST.1943-541X.0002353.
[48] D. Lignos, H. Krawinkler, Deterioration Modeling of Steel Components in Support of Collapse Prediction of Steel Moment Frames under Earthquake Loading, Journal of Structural Engineering. 137 (2011) 1291–1302. https://doi.org/10.1061/(ASCE)ST.1943-541X.0000376.
[49] A. Gupta, H. Krawinkler, Seismic Demands for Performance Evaluation of Steel Moment Resisting Frame Structures, 1999.
[50] A. Skiadopoulos, A. Elkady, D.G. Lignos, Proposed Panel Zone Model for Seismic Design of Steel Moment-Resisting Frames, Journal of Structural Engineering. 147 (2021) 04021006. https://doi.org/10.1061/(ASCE)ST.1943-541X.0002935.
[51] F. Zareian, R.A. Medina, A practical method for proper modeling of structural damping in inelastic plane structural systems, Computers & Structures. 88 (2010) 45–53. https://doi.org/10.1016/j.compstruc.2009.08.001.
[52] Introduction to Boosted Trees — xgboost 1.6.0-dev documentation, (2021). https://xgboost.readthedocs.io/en/latest/tutorials/model.html (accessed November 1, 2021).
[53] F. Pedregosa, G. Varoquaux, A. Gramfort, V. Michel, B. Thirion, O. Grisel, M. Blondel, P. Prettenhofer, R. Weiss, V. Dubourg, J. Vanderplas, A. Passos, D. Cournapeau, M. Brucher, M. Perrot, É. Duchesnay, Scikit-learn: Machine Learning in Python, Journal of Machine Learning Research. 12 (2011) 2825–2830.
[54] T. Hastie, R. Tibshirani, J. Friedman, The Elements of Statistical Learning: Data Mining, Inference, and Prediction, Springer, 2009.
[55] R. Chandramohan, Duration of earthquake ground motion: influence on structural collapse risk and integration in design and assessment practice, Stanford University, 2016. http://purl.stanford.edu/fg920pt3240 (accessed November 2, 2021).
[56] K. Zhong, R. Chandramohan, J.W. Baker, G.G. Deierlein, Site-specific adjustment framework for incremental dynamic analysis (SAF-IDA), Earthquake Spectra. (2022) 87552930221083680. https://doi.org/10.1177/87552930221083688.